This paper was presented as part of the main technical program at IEEE INFOCOM 2011

Optimal Multiple-Coverage of Sensor Networks

Xiaole Bai*, Ziqiu Yun†, Dong Xuan‡, Biao Chen§ and Wei Zhao§

*Department of Computer and Information Science, University of Massachusetts Dartmouth, MA, USA. xbai@umassd.edu
†Department of Mathematics, Soochow University, Suzhou 215006, China. ziqiuyun@gmail.com
‡Department of Computer Science and Engineering, The Ohio State University, Columbus, USA. xuan@cse.ohio-state.edu
§ Department of Computer and Information Science, University of Macau, Macau, P. R. China. {bchen, weizhao}@umac.mo

***Abstract*—In wireless sensor networks, multiple-coverage, in which each point is covered by more than one sensor, is often required to improve detection quality and achieve high fault tolerance. However, finding optimal patterns that achieve multiple-coverage in a plane remains a long-lasting open problem. In this paper, we first derive the optimal deployment density bound for two-coverage deployment patterns where Voronoi polygons generated by sensor nodes are congruent. We then propose optimal two-coverage patterns based on the optimal bound. We further extend these patterns by considering the connectivity requirement and design a set of optimal patterns that achieve two-coverage and one-, two-, and three-connectivity. We also study optimal patterns under practical considerations. To our knowledge, our work is the very first that proves the optimality of multiple-coverage deployment patterns.**

I. Introduction

A. Motivation

Wireless Sensor Network (WSN) deployments with higher degrees of sensing coverage are important. Sensing coverage is closely coupled with monitoring quality. Some applications require multiple-coverage to achieve their goals, e.g., distributed target detection, data fusion, and classification [17], [23]. Moreover, multiple-coverage yields higher fault tolerance in the face of node failures.

Designing proper topology control and scheduling algorithms to achieve multiple-coverage in WSNs has attracted intensive research. However, one important cornerstone is still missing: *what are the deployment patterns that use the minimum number of sensor nodes to cover every point of a region with at least k sensors (k-covered) for $k > 1$?* This problem is also known as the optimal multiple-coverage problem.

Fundamentally, knowledge of optimal multiple deployment patterns will help reduce the number of required sensor nodes and their cost by avoiding ad-hoc and potentially inefficient deployments. It can also provide theoretical guidance and performance measures for heuristic algorithms that are developed for topology control. Furthermore, such knowledge can help in designing practical guidelines for minimizing message collisions, improving network management, routing, etc. They will also provide guidelines in non-ideal and more practical sensor deployment scenarios involving non-uniform communication/sensing ranges, non-uniformity with respect to hierarchical networks, certain gateway nodes, deployment fields, etc. It is noteworthy that studying optimal multiple-coverage patterns can help establish theoretical foundations and practical guidelines for not only WSNs, but also other wireless networks, such as mesh and cellular networks. For instance, the resulting optimal patterns can be directly applied to the deployment of access points (APs) in mesh networks and base stations (BSs) in cellular networks. In addition, the research results will broaden our understanding of the applications of geometry with respect to computer networks. In fact, the optimal one-coverage problem has already been intensively studied in recent years [1], [12], [24], [30].

The optimal multiple-coverage problem is related to the disk covering problem in the field of geometry. Notably, Kershner solved the optimal one-coverage problem in 1939 [15]. Kershner proved that the triangle lattice pattern is the optimal pattern that achieves one-coverage. *The deployment density of the triangle lattice pattern is* $2\pi/3\sqrt{3}$.[1] However, the optimal multiple-coverage problem remains an open problem to date. In this paper, we study the optimal two-coverage problem as a first step to tackle this open problem.

B. Contributions

We highlight our two major contributions as follows.

– *Optimal Patterns to Achieve Two-Coverage.* In this paper, for the first time, we provide the deployment density with proved optimality for two-coverage deployment patterns. Specifically, we consider the deployment density of congruent deployments where Voronoi polygons generated by sensor nodes are congruent. We prove that:

The deployment density for all possible congruent deployments that achieve two-coverage is at least $4\pi/3\sqrt{3}$.

To the best of our knowledge, our results are the first direct answers to the optimal multiple-coverage problem. We are now able to construct two-coverage deployment patterns with proved optimality. In the triangle lattice pattern that

†Corresponding author; this work was supported in part by the National Science Foundation of China (NSFC) under grant No. 61070245 and No. 10971185. ‡This work was supported in part by the US National Science Foundation (NSF) CAREER Award CCF0546668, CNS0916584 and the Army Research Office (ARO) under grant AMSRD-ACC-R50521-CI. §This work was supported in part by China 973 Project 2011CB302800. Any opinions, findings, conclusions, and recommendations in this paper are those of the authors and do not necessarily reflect the views of the funding agencies.

[1]The formal definition of deployment density is provided in Section III.

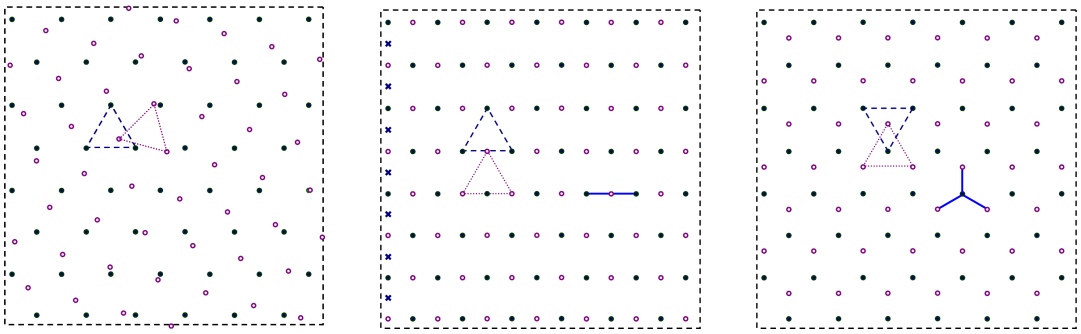

(a) (b) (c)

Fig. 1. Deployment patterns constructed with two layers of triangle lattice patterns (denoted by "•"s and "o"s, respectively). The pattern in Fig.1a is constructed by randomly overlapping the two layers. The deployment pattern in Fig.1b is constructed by first placing each second-layer vertex at the middle of the horizontal edge of each triangle in the first layer and then adding a vertical line of sensor nodes (denoted by "×"s) to connect all horizontal lines. Each sensor node at a horizontal line can communicate with its neighbors in the same line (denoted by the solid line segments). It is one typical optimal two-coverage deployment pattern that achieves one-connectivity. The pattern in Fig.1c is constructed by placing each second-layer vertex at the center of each triangle in the first layer. Each sensor can communicate with its three neighbors (denoted by the solid line segments). It is one typical optimal two-coverage deployment pattern that achieves three-connectivity.

is optimal to achieve one-coverage, the percentage of the overlapping areas is 17.3%.[2] These overlapping areas in the triangle lattice pattern already provide two-coverage. Hence, one might naturally believe that such overlapping areas should be reused in constructing two-coverage deployment patterns. However, notice that the optimal density we obtained is exactly twice the density of the triangle lattice pattern. This implies, surprisingly, that optimal two-coverage deployment patterns do not reuse these overlapping areas in the triangle lattice pattern. Our results show that all deployment patterns constructed by integrating two layers of triangle lattice patterns, no matter how they overlap, have the proved optimal density. Fig. 1a illustrates one such example.

A successful separation from one two-coverage deployment pattern into two one-coverage deployment patterns can avoid reusing overlapping areas, which is a complicated problem, and hence provide much convenience. Although such separation has been assumed and used in existing works, it is solely based on researchers' intuition. For the first time, our results in this paper provide solid theoretical support for this intuition. For example, in the ROAL protocol [16], sensor nodes are first selected to form a one-coverage pattern and this process is repeated twice to eventually achieve two-coverage. Our results provide not only a theoretical basis but also performance measures for such separation-based algorithm designs. In general, our results are valuable to algorithm designs that are based on layer-wise separation to achieve multiple-coverage, such as [5], [9], etc.

– *Optimal Patterns to Achieve Connected Two-Coverage.* In WSNs, connectivity is also an important requirement. Due to our results in this paper, it now becomes possible to obtain different two-coverage deployment patterns with various degrees of connectivity by controlling the relative locations of two separated layers of one-coverage patterns.

In this paper, we propose a general form for deployment patterns that can achieve two-coverage and one- or two-connectivity when $r_c > \sqrt{3}r_s/2$. This general form contains infinitely many pattern forms, all of which are optimal congruent patterns. Fig. 1b illustrates one example of these patterns that achieve one-connectivity. We also propose a general form for deployment patterns that can achieve two-coverage and three-connectivity when $r_c > r_s$. This general form also contains infinitely many pattern forms, all of which are optimal congruent patterns. Fig. 1c illustrates one deployment pattern example with three-connectivity. Due to the infinite number of optimal connected two-coverage deployment patterns, we can properly choose patterns that meet various practical requirements.

Paper Organization We present related work and some background information in Section II, followed by system models and definitions in Section III. In Section VI, we introduce our new results on optimal two-coverage deployment patterns. In Section V, we consider connected two-coverage. Practical considerations are discussed in Section VI. We conclude the paper in Section VII.

II. Related Work

The optimal deployment pattern problem is fundamental. Related work is scattered throughout both the areas of geometry and WSNs.

In geometry, this problem is related to the covering problem. Covering a set of points using a minimum number of given geometric bodies has been extensively studied for disks in a large area [15], [10], disks on a bounded square [19], [20], orthogonal rectangles [8], fat convex bodies [7], [22], etc. Among these works, the most well-known and widely used result is Kershner's, which states that the triangle lattice pattern is the optimal pattern to achieve one-coverage [15]. However, to the best of our knowledge, one-coverage dominates the geometry literature.

[2]The overlapping area is the difference between the area of a disk and the area of a regular hexagon inscribed in the disk. The regular hexagon is the Voronoi polygon generated by each sensor node in the triangle lattice pattern, which denotes the "real" coverage contribution of each node. The percentage is calculated as $(\pi r^2 - 3\sqrt{3}r^2/2)/\pi r^2 = 17.3\%$.

In the area of sensor networks, optimal deployment patterns to achieve one-coverage and connected one-coverage have been intensively studied. The triangle lattice pattern is optimal to achieve one-coverage and up to six-connectivity when $r_c/r_s \geq \sqrt{3}$. This result is re-proved in [30]. In 2005, the triangle pattern was shown to be non-optimal [24] when $r_c/r_s \geq \sqrt{3}$ is not satisfied; the strip-based pattern can outperform it when $r_c = r_s$ [12]. In 2006, the asymptotic optimality of strip-based patterns to achieve full coverage and one- and two-connectivity was proved in [1] for all ranges of r_c/r_s. In 2008, the asymptotically optimal pattern to achieve full coverage and four-connectivity for $r_c/r_s > \sqrt{2}$ was proposed and proved to be optimal [3]. In [2], a complete set of deployment patterns for all ranges of r_c/r_s to achieve full-coverage and k-connectivity ($k \leq 6$) was proposed. In this set of patterns, those for three- and five-connectivity were proved to be optimal among regular patterns for $r_c/r_s \geq 1$. Optimality is only conjectured for patterns to achieve three- and five-connectivity when $r_c/r_s < 1$, to achieve four-connectivity when $r_c/r_s \leq \sqrt{2}$, and to achieve six-connectivity when $r_c/r_s \leq \sqrt{3}$. The pattern to achieve six-connectivity when $r_c/r_s \leq \sqrt{3}$ was provided and its optimality among regular deployments was proved in [25]. Recently, a pattern mutation phenomenon was discovered among optimal regular deployment patterns when r_c/r_s is small [4].

Considering multiple sensor node coverage, most work focuses on the issue of how to select the minimum number of sensors to be activated from a set of randomly *pre-deployed* sensors such that all interested discrete locations (or targets) are k-covered. This problem is known to be NP-hard [26]. Centralized and distributed approximation algorithms were then proposed [11], [21], [26], [29]. However, no existing work provides any leads toward optimal k-coverage deployment patterns for $k > 1$.

III. Model and Preliminaries

There are several practical sensing models that stem from real device experiments. Megerian *et al.* [18] propose that the sensing quality can be expressed as λ/d^{α}, where λ and α are sensor-dependent parameters and d is the distance between the sensor node and the detection target. In this model, the quality of sensing gradually attenuates with increasing distance. In [27], Zhou *et al.* propose a probabilistic sensing model. In this model, two values R_1 and R_2 ($R_1 \leq R_2$) are defined from empirical observations. When the distance from a target to a sensor node is less than R_1, the target will be detected with probability 1; when the distance is larger than R_2, the detection probability is 0; when the distance is between R_1 and R_2, the detection probability exponentially decreases with increasing distance following the same model as it is presented in [18].

We use the disk model for sensing in this paper. Each sensor is capable of detecting points only within distance r_s. The disk model can be obtained from the above models by first setting a desirable threshold for sensing quality or probability, and then exploiting this threshold to determine the largest possible distance between the sensor and the target. This distance is then chosen to be the sensing range r_s. We notice that for some types of sensors, the sensing capability may vary in different directions. We will discuss this in Section VI. The disk model provides a good abstraction from the real world that has been widely adopted, e.g. in [1], [12]–[14], particularly when certain theoretical foundations are to be established.

We study the asymptotic optimality of deployment patterns, that is, a relatively large area compared with sensing and communication ranges is considered. The boundary effect is not important here and can be ignored. When the region boundaries have to be considered, optimality will vary from case to case as boundary shapes change. We study homogeneous wireless sensor networks where all sensor nodes are identical in terms of sensing.

Definition 3.1: [Voronoi Polygon and Generating Point] Let $\{a_1, a_2, ..., a_p\}$ be a set of p points on a Euclidean plane S. The Voronoi polygon $V(a_i)$ is the set of all points in S, which are closer to a_i (in terms of Euclidean distance) than to any other point, i.e., $V(a_i) := \{x \in S : \forall j \in [1, p], d(x, a_i) \leq d(x, a_j)\}$, and point a_i is the generating point of $V(a_i)$.

If two Voronoi polygons share an edge, their generating points are called neighboring generating points.

Each Voronoi polygon edge resides on the perpendicular bisector of the line segment that connects two neighboring generating points. If there are n edges that intersect at a Voronoi polygon vertex, we say that it is shared by n edges. A vertex in a Voronoi tessellation is shared by at least three edges.

From Lemma 4.1 in [1], the average edge number of a Voronoi polygon in a Voronoi tessellation is not larger than six. Therefore, Voronoi polygons generated in a congruent deployment will have k edges for $k = 3, 4, 5,$ or 6.

Definition 3.2: [k-covered Congruent Deployment] A k-covered congruent deployment is a sensor deployment pattern where the Voronoi polygons generated by sensors are all congruent and every point of the target region is covered by at least k sensors for $k = 1, 2, 3, \ldots$

We call a k-covered congruent deployment a *congruent deployment* for short when the value of k is not important. We call a Voronoi tessellation a *congruent Voronoi tessellation* if the Voronoi polygons in the tessellation are all congruent. Congruent deployments generate congruent Voronoi tessellations with sensor nodes being generating points.

Definition 3.3: [Deployment Density] Deployment density, or density for short, is a ratio of the area of sensing disks to the area of Voronoi polygons generated by sensor nodes.

Since the area of a Voronoi polygon can be considered as the pure contribution to coverage from each sensor node [1], large Voronoi polygon areas imply a small density and a more efficient deployment pattern.

Definition 3.4: [c-Optimal Pattern] A deployment pattern is called c-optimal if its deployment density equals the the minimum density among all two-covered congruent deployments.

From Definition 3.4, a c-optimal pattern is not necessarily a congruent deployment pattern. It is a more general concept. A deployment pattern is called c-optimal as long as its density

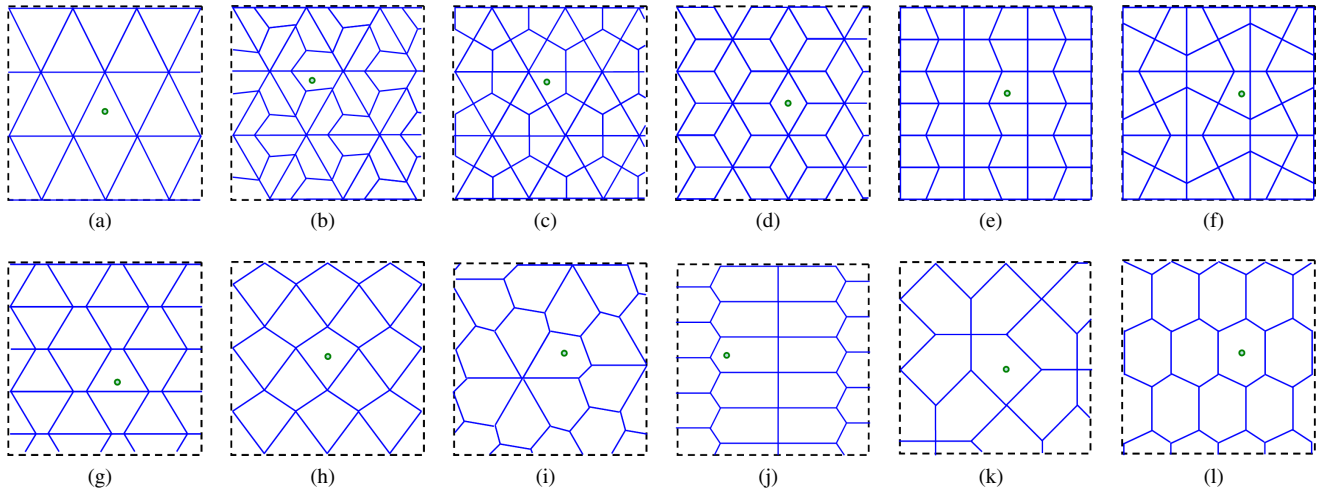

Fig. 2. Voronoi tessellations generated by congruent deployments. Figs. 2a−2l correspond to the 12 types in Lemma 4.1. The small dot in each figure indicates the location of a sensor node, i.e., the generating point, within the Voronoi polygon.

is equal to the density of the optimal two-covered congruent deployment patterns. On the other hand, the optimal two-covered congruent deployment patterns must be c-optimal.

Studying the optimal density of congruent deployments is meaningful from both theoretical and practical views. All proved globally optimal one-coverage patterns, which are optimal among all possible one-coverage patterns, are indeed congruent deployment patterns. Examples include the triangle lattice pattern [15], the strip-based pattern [1], and the diamond pattern [3]. Congruent deployment patterns also have strong practical implications in homogeneous WSNs. Studying c-optimal patterns is an important step toward having globally optimal two-coverage solutions.

IV. Multiple-Coverage

We present our results on two-coverage in this section. The following Theorem 4.1 is the main conclusion.

Theorem 4.1: c-optimal deployment patterns have density $d^* = 4\pi/3\sqrt{3}$.

Theorem 4.1 provides a direct answer to the optimal multiple-coverage problem for the first time by stating that the smallest density for any two-covered congruent deployment is d^*. It also provides a valuable criterion for optimality determination.

The proof of Theorem 4.1 consists of two steps. In the first step, we find all possible congruent Voronoi tessellations that are generated by congruent deployment patterns. In the second step, we prove that the densities of these congruent deployment patterns are at least d^* if two-coverage is achieved. The following subsections IV-A and IV-B detail these steps.

A. Case Reduction

The following Lemma 4.1 summarizes the results of the first step. It states that we can classify all possible congruent Voronoi tessellations into 12 types.

Lemma 4.1: There are 12 types of congruent Voronoi tessellations.

The 12 types of congruent tessellations, types $(a)-(l)$, are shown in Figs. 2a−2l. Due to space limitations, their detailed descriptions are provided in the journal version of this paper. Types $(a)-(l)$ can be divided into two groups. The first group contains types $(c), (d), (i)$ and (k). In this group, each type only contains one specific pattern form, i.e., the inner angles of polygons in each type cannot change once r_s is fixed. The second group contains the remaining types. In this group, each type contains infinitely many pattern forms, i.e., inner angles and edge lengths of polygons in each type can change even if r_s is fixed. For example, both the triangle lattice pattern and the strip-based pattern [1] are special forms of type (l), and both the square pattern (the pattern in which Voronoi polygons are squares) and the rectangle pattern (the pattern in which Voronoi polygons are rectangles) can be special forms of types (e), (f), (g) and (h). Although Voronoi polygons in type (k) patterns apparently are special forms of those in type (j) patterns, these two types are in fact different. In type (k), each Voronoi polygon is a combination of a square and a right angled isosceles triangle, whereas in type (j), we can change the inner angles except two right angles. The relationship between type (c) and type (h) is similar.

The proof of Lemma 4.1 is not trivial and we present it in the Appendix.

B. Bound Derivation

In this section, we prove that there exists a lower bound of all deployment density for all the deployment patterns that can generate one of the 12 types of congruent Voronoi tessellations in Lemma 4.1 and simultaneously achieve two-coverage. The following Lemma 4.2 holds the key to the second step.

Lemma 4.2: The deployment density of any two-covered congruent deployment pattern that can generate one of 12 types of congruent Voronoi tessellations is at least d^*.

Proof: Lemma 4.2 holds clearly for type (a) shown in Fig. 2a, i.e., when the congruent Voronoi tessellation consists of triangles, since the area of a triangle within a disk reaches

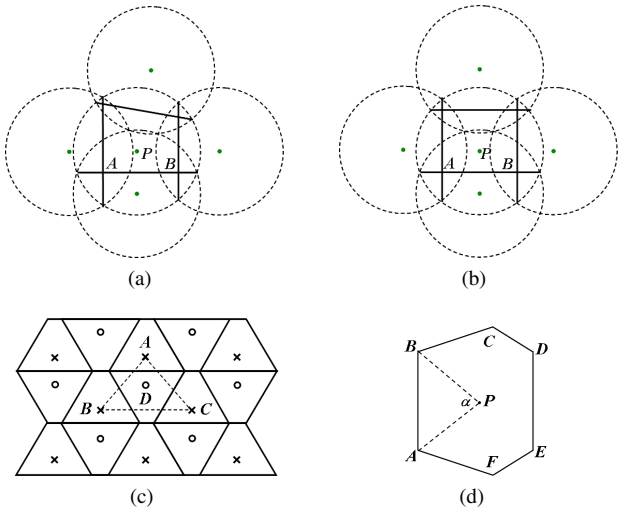

Fig. 3. Reference figures used in the proof of Theorem 4.1. Fig. 3a and 3b are for type (e). Fig. 3c is for type (g) and Fig. 3d is for type (l).

its maximum when it is regular and inscribed in that disk. To prove Lemma 4.2, we need to prove that the density is at least d^* for deployments that generate the remaining 11 types.

To show that the density of each of the remaining 11 Voronoi tessellation types is at least d^* for two-coverage deployments, the proof techniques we use differ depending on types. For types $(e), (f), (j)$ and (k), we need to first transform Voronoi polygons while keeping their areas unchanged, then construct a function of area, and get the minimum value of this function, and finally prove this value is at least d^*. For type (g), we need to divide the two-coverage pattern into two one-coverage patterns. For other types, we just use the geometrical characteristics of these patterns. Due to space limitations, we only present the proofs for three representative cases, each of which corresponds to one type of the aforementioned proof techniques. We present proofs for types (e), (g), and (l). The proofs of other types are presented in the journal version of this paper.

Consider type (e) shown in Fig. 2e. We first transform the Voronoi polygons. We transform the Voronoi polygon that is a right trapezoid to a rectangle where the length of the right leg (AB) and the distance from the generating point (P) to the right leg (AB) are kept unchanged. The area of the rectangle and the right trapezoid are the same. Thus we can focus on the cases where the Voronoi polygons are rectangular.

Since the density will not change when the location of the generating point changes within the Voronoi rectangle, we may consider the case where the generating point is the central point of the rectangle. Denote the length of the short edges of the rectangle by a. Note that, in a two-covered deployment, for each Voronoi polygon generated by a sensor node, there is at least one edge to which the distance from the sensor node is at most $r_s/2$. Hence, we have $a \leq r_s$. Due to the two-coverage requirement, the Voronoi rectangle with generating point P should be fully covered by other four disks with centers P_1, P_2, P_3 and P_4. We can obtain the length of the long edges is $b \leq r_s^2 + \sqrt{r_s^2 - a^2}$. Hence the area of the rectangle is at most $a(r_s^2 + \sqrt{r_s^2 - a^2})$. Let $f(a) = a(r_s^2 + \sqrt{r_s^2 - a^2})$. We can obtain that $f(a)$ achieves its maximum in the range of $[0, r_s]$ when $a = \sqrt{3}r_s/2$. The maximal value is $3\sqrt{3}r_s/4$. Hence, the density is not less than d^*.

Consider type (g) shown in Fig. 2g. As shown in Fig. 3c, we divide generating points into two groups denoted by "$\times$"s and "$\circ$"s. We connect those denoted by small crosses, which partitions the plane into a tessellation of congruent triangles. One such triangle is denoted by ABC in Fig. 3c. Consider triangle ABC. We remove the disk centered at the generating point D within ABC. If we remove any one sensor from a two-covered deployment, the remaining sensor nodes achieve at least one-coverage. Hence, the remaining disks still achieve one-coverage here. Since the minimum distance from any point within triangle ABC to its vertices is at most the distance from the three ABC vertices to any other generating point except D, triangle ABC can be fully covered by three disks centered at the vertices. Note that, given a triangle, a necessary and sufficient condition for the disks with radius r_s centered at its vertices to cover it is that the radius of the circumscribed circle of the triangle is at most r_s. Therefore, all the triangles whose vertices denoted by small crosses are fully covered by disks centered at their vertices. Hence, the entire plane is one-covered by the disks centered at the vertices denoted by small crosses. For exactly the same reason, the entire plane is also one-covered by the disks center at the vertices denoted by small circles. If a two-covered deployment is constructed with two one-coverage layers, its density is at least $4\pi/3\sqrt{3}$. Hence, the density here is at least d^*.

Consider type (l) shown in Fig. 2l. As shown in Fig. 3d, denote the generating point P within polygon $ABCDEF$ by P. Note that, if a vertex O in a Voronoi tessellation is shared by three edges OA, OB, and OC, then $\angle P_1OA + \angle BOC = \pi$, where P_1 is the generating point of the Voronoi polygon that consists of edges OA and OB. Hence, we have $AB||DE$, $AB = DE$, $BC = AF$, and $CD = EF$. Fig. 3d is a Voronoi polygon iff $ABCDEF$ inscribes a disk that is centered at P.

Denote the central angle at P that is opposite to the longest edge of polygon $ABCDEF$ by α. We have $\pi/3 \leq \alpha < \pi$. To achieve 2-coverage, the sensing disk radius r should satisfy $r_s \geq 2\cos\frac{\alpha}{2}$. Hence, $d \geq \pi r_s^2/(\sin\alpha + 2\sin\frac{\pi-\alpha}{2}) \geq 2\pi(\cos\alpha + 1)/(\sin\alpha + 2\cos\frac{\alpha}{2})$. Since $f(\alpha) = \sin\alpha + 2\cos\frac{\alpha}{2}$ is a monotone decreasing function at range $[\pi/3, \pi)$, we have $d > 2\pi/\frac{3\sqrt{3}}{2} = d^*$. ■

C. Remarks

Since the lower bound d^* obtained in Lemma 4.2 is achievable, e.g., by integrating two layers of triangle lattice patterns, d^* is the optimal density of two-covered congruent deployment patterns. Theorem 4.1 then holds directly. We also conjecture that this density d^* is actually a globally optimal density since all proved one-coverage optimal patterns are indeed congruent deployment patterns, as we mentioned before in Section III.

Based on Theorem 4.1, it now becomes possible to determine optimality for multiple-coverage deployments. The following

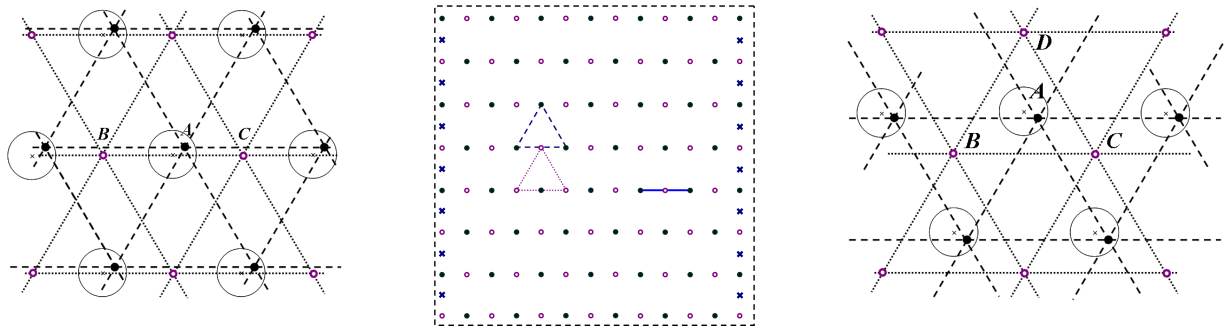

(a) (b) (c)

Fig. 4. A general form of one- or two-connected c-optimal deployment patterns is presented in Fig. 4a. The pattern in Fig. 4b is a specific form of two-connected c-optimal patterns which consists of two layers of the triangle lattice patterns (denoted by "•"s and "○"s respectively). It is constructed by first placing each second layer vertex at the middle of the horizontal edge of each triangle of the first layer and then adding two sensor node vertical lines (denoted by "×"s) to connect all horizontal lines at the both boundaries. Each sensor node at a horizontal line can communicate with its neighbors in the same line (denoted by solid line segments). Fig. 4c presents a general form of three-connected c-optimal deployment patterns.

Theorem 4.2 provides theoretical support by stating the optimality for arbitrarily overlapping of two layers of triangle lattice patterns. Its proof is straightforward and omitted here.

Theorem 4.2: All deployments constructed with two layers of triangle lattice patterns are c-optimal.

We can naturally obtain another important conclusion in Theorem 4.3. Theorem 4.3 states that, among all two-covered congruent deployments, those constructed with two layers of triangle lattice patterns are optimal.

Theorem 4.3: All congruent deployment patterns constructed with two layers of triangle lattice patterns are optimal congruent deployment patterns.

There are infinitely many congruent deployments as long as triangle edges in different layers are parallel. Hence, we have infinitely many optimal two-covered congruent deployments. This contrasts with the one-coverage case where it is widely believed that the triangle lattice pattern is the unique optimal congruent deployment.

V. Connected Multiple-Coverage

In WSNs, connectivity is also important. We use the disk model for communication, i.e., each sensor node is capable of communicating only with others within distance r_c. The disk model is widely used in the literature [1], [12], [24], [30]. It can be considered a simplified version of the real models, e.g., the one proposed by Zuniga *et al.* [28]. They suggest communication link quality can be measured by the packet reception rate (PRR). The PRR at distance d is $(1 - exp(-\frac{P_t - PL(d) - P_n}{2})/2)^{8\ell}$, where P_t is the output power of the transmitter, $PL(d)$ is the path loss at distance d, P_n is the noise floor, and ℓ is the frame length. The disk model considers a connection established between two sensor nodes only if the PRR from each other is above a certain threshold.

Our results in Section IV provide a basis to design connected c-optimal patterns. To obtain different degrees of connectivity, our approach consists of two steps. The first step is to design the relative position of two layers of triangle lattice patterns according to the relationship between r_c and r_s. The second step is to integrate the two layers together. From Theorem 4.2, the deployment patterns constructed in this way are all c-optimal.

Due to space limitations, we will skip the obvious cases, e.g., 12-connectivity can be achieved when vertices of two triangle lattice layers entirely overlap and $r_c/r_s \geq \sqrt{3}$. In the following, we present general forms of two-coverage deployment patterns that achieve one-, two-, and three-connectivity, respectively.

A. Optimal One- or Two-Connected Two-Coverage Patterns

In this section, we present one- or two-connected c-optimal patterns for $r_c > \sqrt{3}r_s/2$.

The general form of optimal patterns can be illustrated by showing how they are constructed. To obtain such patterns, we integrate two triangle lattice layers as shown in Fig. 4a. In each layer, we first let each triangle have a horizontal edge, e.g., edge BC, and then make a small disk with radius $r_c - \sqrt{3}r_s/2$ that is centered at the middle point (denoted by "×"s) of the horizontal edge. We then let each triangle in the other layer also have a horizontal edge and each vertex (denoted by "•"s) be within each small disk in the first layer.

In the final deployment pattern we construct, the distance between any vertex in the second layer, e.g., node A, and the corresponding vertices in the first layer, e.g., nodes B and C, are both less than r_c. Hence, such deployment can achieve two-coverage and one-connectivity when one vertical line of sensor nodes are deployed to connect all horizontal sensor node lines, and two-connectivity if two vertical lines of sensor nodes are deployed to connect all horizontal lines at the both boundaries.

A typical two-coverage and one-connectivity deployment pattern is shown in Fig. 1b, and a typical two-connectivity pattern is shown in Fig. 4b. In these two specific deployment patterns, one- or two-connectivity also holds for $r_c = \sqrt{3}r_s/2$.

B. Optimal Three-Connected Two-Coverage Patterns

In this section, we present three-connected c-optimal patterns for $r_c > r_s$.

Again, we will explain how to construct the general form of such optimal patterns. Two triangle lattice layers are integrated

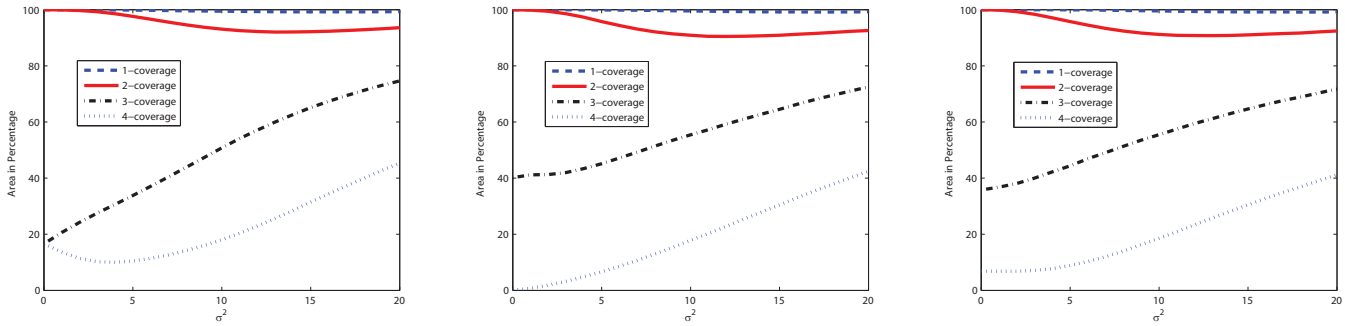

(a) (b) (c)

Fig. 5. Coverage under sensing irregularity for three different typical deployment patterns. Fig. 5a is for the case when the vertices of two triangle lattice layers entirely overlap. Fig. 5b is for the case when the deployment pattern shown in Fig. 1c. Fig. 5c is for the case when the deployment pattern shown in Fig. 1b (or Fig. 4b) but without vertical sensor lines.

in the following way as illustrated in Fig. 4c. In one layer, we make small disks with radii $r_c - r_s$ that are centered at the central points of triangles (denoted by "$\times$"s). We then let the vertices of another layer (denoted by "$\bullet$"s) fall into the small disks and let the corresponding triangle edges in different layers be parallel. The maximal distances between any vertex in the second layer, e.g., node A, and the three vertices in the first layer that form a triangle enclosing the vertex in the second layer, e.g., nodes B, C, and D, are less than r_c.

One two-coverage three-connectivity pattern is shown in Fig. 1c. In this pattern, three connectivity also holds for $r_c = r_s$.

C. Remarks

We present both one- and two-connected c-optimal deployment patterns here since they have the minimal requirement on the r_c range (over r_s) for networks to be connected. However, the long-path problem, i.e., a message transmitted between two sensor nodes that are close to each other but on different horizontal lines has to get over a long distance, may exist in some applications using these patterns. To overcome this, we propose three-connected c-optimal deployment patterns as above. Note that the connection links in the three-connected deployment patterns are evenly distributed over the network.

Note that, when $r_c > \sqrt{3}r_s/2$, there are infinitely many one- or two-connected c-optimal deployment patterns. When $r_c > r_s$, there are also infinitely many three-connected c-optimal deployment patterns. We can take advantage of the infinite variants of the patterns to meet different design requirements. For example, when three-connectivity and large distances between sensor nodes are needed to improve proper traffic balancing and reduce interference, placing the second layer vertices at the centers of the triangles in the first layer can be a preferred type.

VI. Practical Issues

In reality, the sensing range may not exactly follow the disk sensing model. Megerian *et al.* [18] propose that sensing quality gradually attenuates with distance. Zhou *et al.* [27] propose a probabilistic sensing model where the detection probability varies with different target distances. When the above models are used, the sensing disk can be obtained by setting a sensing range threshold that is based on a desirable sensing quality or detection probability. In some cases, the sensing area is non-disk even after a threshold has been set. Cao *et al.* [6] suggest the sensing capability roughly follows a Gaussian distribution over different directions. Denote the average sensing radius over all directions by μ and the standard deviation by σ^2. As σ decreases, the sensing field is more like a disk.

We study by simulation the impact from such sensing irregularity on the previously-discussed c-optimal deployment patterns that are constructed with two layers of triangle lattice patterns. We study three typical cases: case 1) when vertices of two triangle lattice layers entirely overlap; case 2) when vertices of the second triangle lattice layer are located at the center of the triangles in the first layer, as shown in Fig. 1c; and case 3) when triangles in both layers have horizontal edges and the vertices of the second triangle lattice layer are located at the middle of the horizontal edges in the first layer, as shown in Fig. 1b or 4b. In our simulation, sensor nodes are deployed over a $1,000$ m $\times$ $1,000$ m region. Each sensor node has a 30 m average sensing range in each direction ($\mu = 30$ m) with variance σ^2 ranging from 0 to 20. In each simulation, we randomly generate $100,000$ points in the deployment region and then check their coverage. We repeat simulations with the same configuration for μ and σ^2 500 times and then take the average.

The respective results are shown in Fig. 5a, Fig. 5b, and Fig. 5c. In these figures, "k-coverage" means at least k-covered. We observe from the figures that performance under irregularity for all three cases is close when sensing ranges are highly irregular. This indicates that sensor node location information plays an insignificant role at this time. However, there are salient differences when sensing ranges are quite regular, especially when $\sigma^2 \leq 5$. In cases 2 and 3, there is a higher percentage of areas that are covered by at least three sensors than that in case 1. In case 1, there are more areas that are covered by at least four sensors. Such differences turn out to be negligible as

irregularity increases. Interestingly, we observe some convex curves, e.g., the one showing the percentage of four-covered area in case 1. This phenomenon occurs since proper sensor locations with regular sensing disks as well as irregular sensing ranges with not-so-important relative locations can both help achieve a high degree of coverage. The transition between these two yields a temporary decrease of highly covered area.

We also observe that, in practice, the communication model may not follow the disk model. Furthermore, in real-world deployments, deployment errors and dominating geographical constraints of the deployment region must also be taken into account. In some cases, hierarchical sensor network architectures are desirable. Serving as a fundamental reference, our optimal deployment patterns presented in this paper are still essential when these practical issues are addressed. Due to space limitations, we omit further discussion of these issues in the paper. We refer the interested reader to [1]–[4], [25] for detailed discussions.

VII. Conclusions

WSN deployments with higher degrees of sensing coverage are important. Finding optimal patterns that achieve multiple-coverage with the minimum number of sensor nodes is a fundamental but difficult problem that remains unsolved to date. In this paper, we study c-optimal patterns. To the best of our knowledge, this paper makes the first step towards finding the ultimate solutions to the optimal multiple-coverage problem. Our results have both theoretical and practical significance. Our future work focuses on considering globally optimal multiple-coverage patterns and extending our patterns to non-disk-based sensing and communication models.

References

[1] X. Bai, S. Kumar, D. Xuan, Z. Yun and T. Lai. Deploying Wireless Sensors to Achieve Both Coverage and Connectivity. In *Proc. of ACM MobiHoc,* 2006.

[2] X. Bai, D. Xuan, Z. Yun, T. Lai and W. Jia. Complete Optimal Deployment Patterns for Full-Coverage and k-Connectivity (k $\leq$6) Wireless Sensor Networks. In *Proc. of ACM MobiHoc,* 2008.

[3] X. Bai, Z. Yun, D. Xuan, T. Lai and W. Jia. Deploying Four-Connectivity And Full-Coverage Wireless Sensor Networks. In *Proc. of IEEE INFOCOM,* 2008.

[4] X. Bai, Z.Yun, D. Xuan, W. Jia and W. Zhao. Pattern Mutation in Wireless Sensor Deployment. In *Proc. of IEEE INFOCOM,* 2010.

[5] J. Cho, S. Kwon, J. Ko, and C. Kim. An efficient multilevel coverage scheme in mobile sensor networks. In *Proc. of ISWPC,* 2009.

[6] Q. Cao, T. Yan, J. Stankovic and T. Abdelzaher. Analysis of Target Detection Performance for Wireless Sensor Networks. In *Proc. of DCOSS,* 2005.

[7] K. Clarkson and K. Varadarajan. Improved Approximation Algorithms for Geometric Set Cover. *Discrete & Computational Geometry,*vol. 37, no. 1, pp. 43-58, 2007.

[8] T. Gonzalez. Covering a Set of Points in Multidimensional Space. *Information Processing Letters,*vol. 40, no. 4, pp. 181-188, 1991.

[9] A. Gallais , J. Carle , D. Simplotryl , and I. Stojmenovic. Ensuring Area k-Coverage in Wireless Sensor Networks with Realistic Physical Layers. In *Proc. of IEEE SENSORS,* 2006.

[10] D. Hochbaum and W. Maass. Approximation Schemes for Covering and Packing Problems in Image Processing and VLSI. *Journal of the ACM,* vol. 32, no. 1, pp. 130-136, 1985.

[11] M. Hefeeda and M. Bagheri. Randomized k-Coverage Algorithms For Dense Sensor Networks. In *Proc. of IEEE INFOCOM,* 2007.

[12] R. Iyengar, K. Kar and S. Banerjee. Low-coordination Topologies for Redundancy in Sensor Networks. In *Proc. of ACM MobiHoc, 2005.*

[13] S. Kumar, T. Lai, and J. Balogh, On k-Coverage in a Mostly Sleeping Sensor Network. In *Proc. of ACM MobiCom,* 2004

[14] S. Kumar, T. Lai, and A. Arora, Barrier Coverage With Wireless Sensors. In *Proc. of ACM MobiCom,* 2005

[15] R. Kershner. The Number of Circles Covering a Set. *American Journal of Mathematics,* vol. 61, pp. 665-671, 1939.

[16] H. Kim, E. Kim, and K. Yum. ROAL: A Randomly Ordered Activation and Layering Protocol for Ensuring K-Coverage in Wireless Sensor Networks. *Journal Of Networks,* vol. 3, no. 1, pp. 43–52, 2008.

[17] D. Li, K. Wong, Y. Hu, and A. Sayeed. Detection, Classification and Tracking of Targets in Distributed Sensor Networks. *IEEE Signal Processing Magazine,* vol. 19, no. 2, 2002.

[18] S. Megerian, F.Koushanfar, G. Qu, G. Veltri and M. Potkonjak. Exposure in Wireless Sensor Networks: Theory and Practical Solutions. *Wireless Networks,* vol. 8, no. 5, 443-454 2002.

[19] J. Melissen and P. Schuur. Improved Coverings of a Square with Six and Eight Equal Circles. *Electronic Journal of Combinatorics,* vol. 3, no. 1, 1996.

[20] K. Nurmela and P. Östergård. Covering a Square with Up to 30 Equal Circles. *Research Report A62, Laboratory for Theoretical Computer Science, Helsinki University of Technology,* 2000.

[21] G. Simon, M. Molnár, L. Gönczy, and Bernard Cousin. Dependable k-coverage Algorithms for Sensor Networks. In *Proc. of IMTC,* 2007.

[22] G. Toth. Covering with Fat Convex Discs. *Journal of Discrete and Computational Geometry,* vol. 34, no. 1, pp. 129-141, 2005.

[23] P. Varshney. Distributed Detection and Data Fusion. *Spinge,* 1996

[24] Y. Wang, C. Hu, and Y. Tseng. Efficient Deployment Algorithms for Ensuring Coverage and Connectivity of Wireless Sensor Networks. In *Proc. of WICON,* 2005.

[25] Z. Yun, X. Bai, D. Xuan, T. Lai, and W. Jia. Complete Optimal Deployment Patterns for Full-Coverage and k-Connectivity ($k \leq 6$) Wireless Sensor Networks. *IEEE/ACM Transactions on Networking,* vol. 18, no. 3, pp. 934-947, 2010.

[26] S. Yang, F. Dai, M. Cardei, and J. Wu. On Connected Multiple Point Coverage in Wireless Sensor Networks. *Journal of Wireless Information Networks,* May, 2006.

[27] Y. Zhou and K. Charkrabarty. Sensor Deployment and Target Localization Based on Virtual Force. In *Proc. of IEEE INFOCOM,* 2003.

[28] M. Zuniga and B. Krishnamachari. Analyzing the Transitional Region in Low Power Wireless Links. *Technical Report.* University of Southen California, 2004.

[29] Z. Zhou, S. Das, and H. Gupta. Connected K-coverage Problem in Sensor Networks. In *Proc. of ICCCN,* 2004.

[30] H. Zhang and J. Hou. Maintaining Sensing Coverage and Connectivity in Large Sensor Networks. In *NSF International Workshop on Theoretical and Algorithmic Aspects of Sensor, Ad Hoc Wirelsss, and Peer-to-Peer Networks,* 2004.

Appendix

In this appendix, we provide a proof sketch for Lemma 4.1. We start our proofs with the following lemmas.

Lemma 7.1: In a Voronoi tessellation, the structure shown in Fig. 6a cannot exist unless two line segments are perpendicular to each other.

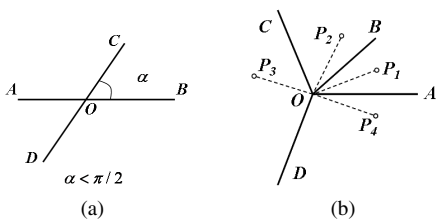

Fig. 6. (a) Impossible structure in a Voronoi tessellation when $\alpha < \pi/2$. (b) P_1, P_2, P_3 and P_4 are generating points. Solid lines are edges of Voronoi polygons generated by them.

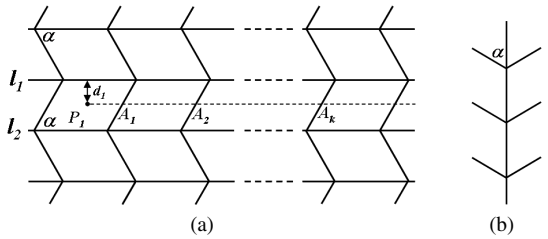

Fig. 7. A tessellation that consists of quadrilaterals where $l_1 || \ l_2$ and $\alpha < \pi/2$.

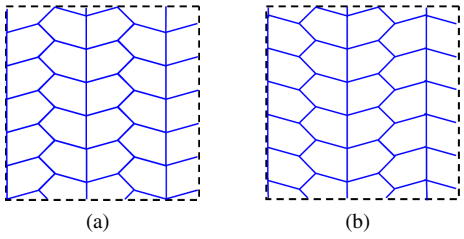

Fig. 8. Reference figures for Lemma 7.5.

Lemma 7.2: If a vertex O in a Voronoi tessellation is shared by four edges, the opposite angles with O as their vertex are complementary.

Proof: We have $\angle P_1OB = \angle P_2OB$, $\angle P_2OC = \angle P_3OC$, $\angle P_3OD = \angle P_4OD$, and $\angle P_4OA = \angle P_1OA$. Hence, $\angle AOB + \angle COD = \angle BOC + \angle DOA$. Since $\angle AOB + \angle COD + \angle BOC + \angle DOA = 2\pi$, $\angle AOB + \angle COD = \angle BOC + \angle DOA = \pi$. ■

Lemma 7.3: If a congruent Voronoi tessellation consists of quadrilaterals, no vertex is shared by five edges or k edges for $k > 6$.

Proof: Denote the four angles in order of a Voronoi quadrilateral by $\alpha_1, \alpha_2, \alpha_3$ and α_4 corresponding to vertices a, b, c and d. From Lemma 4.1 in [1], the average number of edges shared by one vertex is four. If there are vertices that are shared by five edges, then there should be the same number of vertices that are shared by three edges. There are three angles at a vertex when this vertex is shared by three edges. The sum of them is 2π. Since all of them are taken from angles $\alpha_1, \alpha_2, \alpha_3$ and α_4, two of the three angles must be the same since $\alpha_1 + \alpha_2 + \alpha_3 + \alpha_4 = 2\pi$. Without loss of generality, we denote the three angles are α_1, α_1, and α_2. In the following, we first show there cannot be any vertex that is shared by four edges when there are vertices that are shared by five edges and three edges. From $\alpha_1 + \alpha_2 + \alpha_3 + \alpha_4 = 2\pi$ and $2\alpha_1 + \alpha_2 = 2\pi$, we have $\alpha_1 = \alpha_3 + \alpha_4$. Hence, $2\alpha_1 \neq \pi$, $\alpha_1 + \alpha_2 \neq \pi$, and $\alpha_3 + \alpha_4 \neq \pi$. If there are vertices that are shared by four edges, from Lemma 7.2, there are three cases for the two pairs of complementary opposite angles at such vertices: (1) α_1, α_3 and α_2, α_4, or α_1, α_4 and α_2, α_3, (2) α_2, α_2 and α_1, α_3, or α_2, α_2 and α_1, α_4, and (3) α_2, α_2 and α_3, α_3, or α_2, α_2 and α_4, α_4. From case (1), it is easy to have $\alpha_3 = \pi/2$ and $\alpha_4 = 0$, which is impossible. Similarly, case (2) and case (3) are also impossible. When the three angles at the vertex shared by three edges are denoted by α_1, α_1 and α_2, then the five angles at the vertex shared by five edges are α_2, α_3, α_3, α_4, and α_4. We have two cases for the order of these five angles: (1) $\alpha_2\alpha_3\alpha_4\alpha_3\alpha_4$ or $\alpha_2\alpha_4\alpha_3\alpha_4\alpha_3$, and (2) $\alpha_2\alpha_3\alpha_3\alpha_4\alpha_4$ or $\alpha_2\alpha_4\alpha_4\alpha_3\alpha_3$. The proofs for impossibility of these two cases are the same. Consider case (1). Consider the Voronoi quadrilateral that contains α_2. The neighboring edges of α_2 in this quadrilateral is ab and bc. Since ab is actually edge ca or cb of the Voronoi quadrilateral on the other side of ab, the length of ab is equal to ca or cb. Similar analysis applies to bc. Then all Voronoi quadrilaterals are rhombi and then $\alpha_1 + \alpha_2 = \pi$. As $2\alpha_1 + \alpha_2 = 2\pi$, we have $\alpha_1 = \pi$ and $\alpha_2 = 0$, which is impossible. The proof of the case when there is no vertex that is shared by k edges for $k > 6$ is similar. ■

Lemma 7.4: The tessellation shown in Fig. 7a is not a congruent Voronoi tessellation. (Any congruent Voronoi tessellation will not contain the structure shown in Fig. 7b.)

Proof: Assume the tessellation shown in Fig. 7 is a congruent Voronoi tessellation. Take a Voronoi parallelogram between lines l_1 and l_2 and assume its generating point is P_1. Denote the dashed line that goes through P_1 and is parallel to l_1 by l. l intersects edges to the right side of P_1 at points $A_1, A_2, \cdots, A_k$. Denote the edges on which A_k is by e_k. We can then denote a point that is the symmetry point of P_1 about edge e_1 by P_2, a point that is the symmetry point of P_2 about edge e_2 by P_3, $\cdots$, a point that is the symmetry point of P_k about edge e_k by P_{k+1}. From the definition of Voronoi polygon, P_k, $k \geq 2$, are the generating points of Voronoi parallelogram with edges e_{k-1} and e_k. Now we have $|P_1P_{2n+1}| = 2na \sin\alpha$. Denote the distance between P_k and l_1 is d_k. Then, $d_{2n+1} = |P_1P_{2n+1}| \cos\alpha + d_1 = d_1 + na|\sin 2\alpha|$. Notice $d_{2n+1} \to \infty$ as $n \to \infty$. Hence, there is some n that places P_n outside of the area between l_1 and l_2. This contradicts to P_k being a generating point for any $k \geq 2$. ■

From Lemma 7.3, in a congruent Voronoi tessellation consisting of Voronoi quadrilaterals, there are three cases for the vertices to be shared by edges. (1) In one tessellation, some vertices are shared by six edges, some by four edges, and some by three edges. (2) In one tessellation, some vertices are shared by six edges, the others are shared by three edges. (3) In one tessellation, all vertices are shared by four edges. Combining Lemma 7.1−7.4, we have the following proposition.

Proposition 7.1: If the Voronoi polygons generated in a congruent deployment are quadrilaterals, there are seven types of tessellations. They are shown in Figs. 2b−2h.

Proposition 7.2: If the Voronoi polygons generated in a congruent deployment are pentagons, there are three types of tessellations. They are shown in Figs. 2i−2k.

Lemma 7.5: The tessellations shown in Fig. 8a and Fig. 8b are not congruent Voronoi tessellations.

If the Voronoi polygons generated in a congruent deployment are hexagons, then in the tessellation one vertex can be only shared by three edges. We then have the following proposition.

Proposition 7.3: If the Voronoi polygons generated in a congruent deployment are hexagons, there is one tessellation shown in Fig. 2l.

Lemma 4.1 is the combination of Propositions 7.1− 7.3.